Investigation of the rate dependences of the stress of plastic flow and fracture of Mn2-Si steel at normal and elevated temperatures

© G.I. Kanel,[1] G.V. Garkushin,[1,2] A.S. Savinykh,[1,2] S.V. Razorenov,[1,2] S.A. Atroshenko[3]

[1] Joint Institute for High Temperatures, Russian Academy of Sciences,
125412 Moscow, Russia
[2] Institute of Problems of Chemical Physics, Russian Academy of Sciences,
142432 Chernogolovka, Moscow oblast, Russia
[3] Institute of Problems of Mechanical Engineering, Russian Academy of Sciences,
199178 St. Petersburg, Russia
e-mail: garkushin@ficp.ac.ru

The Hugoniot elastic limit and spall strength of reactor Mn2-Si steel under shock compression were measured by recording and subsequent analysis of the wave profiles. The temperature-rate dependences of the resistance to high-strain rate and fracture of steel at normal and elevated temperatures are determined. The results of measurements of the strength characteristics of steel under spall are supplemented by a metallographic analysis of the fracture zone and compared with data for 15Kh2NMFA reactor steel and Armco iron.

Keywords: ferrite-pearlite steel, shock waves, deformation, temperature, Hugoniot elastic limit, spall strength.

Introduction

For storage and transportation to the place of spent nuclear fuel processing, metal concrete containers are currently used, the metal elements of which consist of rolled sheets, ring forgings (coamings), plate forgings and other elements made of low-alloy silicon-manganese Mn2-Si steel of high purity in terms of harmful impurities [1]. This steel is also widely used for various parts and elements of metal structures operating at temperatures from -70 to $+425°$C under pressure. The study of the dynamic strength characteristics of ferrite-pearlite silicon-manganese Mn2-Si steel is stimulated by the need to predict the consequences of intense impacts of natural, man-made or terrorist nature on nuclear power structures [2]. Mathematical models and defining relations used in the calculated prediction of the impact, explosion and other intense pulse effects are based on experimental data on the strength behavior of structural materials at strain rates in the range $10^3 - 10^6 \, \mathrm{s}^{-1}$. There are also academic questions regarding the influence of temperature and strain rate on the resistance to plastic deformation and fracture of steels and alloys. The first of them is related to the ratio of the dynamic strength of the material to its dynamic yield strength. Although in many cases materials with higher spall strength (tensile strength realized under shock-wave loading) have higher values of the Hugoniot elastic limit, this correlation is not universal. The second important issue is related to the influence of temperature on the resistance to high-rate deformation and facture. In connection with the existing uncertainty, it is of interest to accumulate experimental data and compare them for steels and alloys with different strength properties [3–5].

This paper presents the results of studies of the dynamic strength of low-alloy ferrite-pearlite Mn2-Si steel at normal and elevated temperatures in the sub-microsecond range of the duration of the shock load.

1. The material under study

Studies have been conducted with low-alloyed ferrite-pearlitic silicon-manganese Mn2-Si steel the chemical composition of which is given in Table 1. Samples with a thickness from 0.17 to 4 mm were cut from a sheet forged shell by an electroerosion technique. The forged shell was previously subjected to heat treatment, which consisted of quenching from $930°$C into water, followed by tempering at $660 - 670°$C and cooling in air. Mn2-Si steel after heat treatment had a ferrite-pearlite structure with a fine-grained structure, the grain size was $15 - 30 \, \mu$m. According to reference data, the yield strength of steel $\sigma_{0.2}$ at room temperature after quenching and tempering is $315 - 365$ MPa, tensile strength $450 - 490$ MPa. With an increase in temperature to $500°$C, the yield strength drops to 180 Mpa, and the tensile strength — to 360 Mpa.

Since the steel is low-alloy, when processing experimental data for room temperature, an impact adiabat of α-iron with a density of $\rho_0 = 7.85 \, \mathrm{g/cm}^3$ and a longitudinal sound velocity of $c_l = 5.9$ km/s in the form $U_S = 4.63 + 1.33 u_p$, where U_S — the velocity of the shock wave, u_p — the particle velocity constructed from the experimental data

Table 1. Chemical composition of Mn2-Si steel

Content of elements, %												
C	Si	Mn	P	S	Cr	Ni	V	Ti	Al	Nb	N	As
0.08	0.6	1.56	0.008	0.003	0.1	0.23	0.04	0.004	0.032	0.05	0.01	0.008
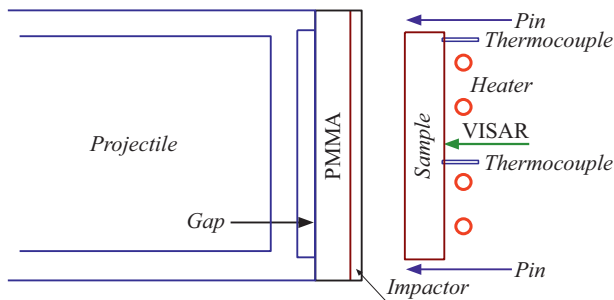
Figure 1. Experimental assembly scheme.

given in [6] data, and for 600°C, taking into account the temperature dependencies of sound velocities [7,8] — in the form of $U_S = 4.37 + 1.33u_p$; the density and longitudinal sound speed under these conditions were 7.66 g/cm³ and 5.5 km/s, respectively.

2. Experimental setup

The experiments were carried out on a stand including a gas gun with a caliber of 50 mm to generate shock compression pulses in the samples under study and a laser Doppler interferometric velocmeter VISAR [9] with a time resolution of ~ 1 ns to record the evolution of compression waves formed by the shock. The experimental scheme is shown in Figure 1. Flat pins made of copper or tungsten with a thickness of 0.04 to 2 mm were glued to a substrate of polymethylmethacrylate with a thickness of 5 mm, located at the end of a hollow duralumin (D16T) projectile. The use of a substrate makes it possible to avoid deflection of thin pins during the acceleration of the latter in the barrel of the gun. The throwing speed was varied by the selection of the pressure of the working gas (air or helium) and was in these experiments 340 ± 10 m/s or 590 ± 20 m/s. The measurements were carried out at room temperature and increased to 600−610°C temperatures of the samples. In the latter case, resistive heaters located at a distance of 2−2.5 mm from the back surface of the sample were used. The temperature was controlled by two chromel-alumel thermocouples with an accuracy of ±3°C. The heating time of the samples, as a rule, was 600 ± 30 s. The impact velocity measurements were carried out using electrical contact sensors (Pin) only in experiments without heating the samples. All experiments were carried out under vacuum.

In addition to shock-wave experiments with the registration of wave profiles, metallographic studies of the spall facture zone of samples preserved after shock compression on transverse sections using an Axio Observer Z1M optical microscope in a light field and in contrast C-DIC after etching in nital (4% solution of HNO_3 in alcohol).

3. Measurement results

Figure 2 shows the results of experiments with samples of Mn2-Si steel of nominal thickness 4 and 2 mm, and Figure 3 — photographs of diametrical cross sections of samples in the area of spallation. Experiments at room temperature were carried out with two ratios of the thickness of the impactor and the sample — 1/2 and 1/4. In Western, primarily American studies, as a rule, pins with a thickness equal to half the thickness of the sample are used. This thickness ratio leads, as will be discussed below, to an additional error in determining the value of the spall strength.

On the velocity profiles of the free surface, the output of an elastic precursor (elastic compression wave, the first „step"), a plastic shock wave, the region of constancy of parameters following it („plateau") and then a part of the rarefaction wave are sequentially recorded. The duration of the plateau is determined by the reverberation time of the waves in the impactor and, accordingly, the greater it is, the greater the thickness of the impactor. The velocity of propagation of the elastic precursor is almost equal to the longitudinal speed sound $c_l = \sqrt{(K + 4G/3)/\rho}$, and the velocity of the plastic shock wave is determined by the bulk compressibility of the material and, accordingly, is close to the bulk speed of sound $c_b = \sqrt{K/\rho}$ [10,11] at moderate shock compression amplitudes.

The amplitude of the elastic precursor is determined by the Hugoniot elastic limit of the material HEL (Hugoniot elastic limit) and is equal to

$$\sigma_{\text{HEL}} = 0.5u_{\text{HEL}}\rho_0 c_l, \tag{1}$$

where u_{HEL} — free surface velocity jumps in the precursor. The elastic limit under one-dimensional deformation is related to the yield strength in the usual sense of σ_T by the ratio

$$\sigma_T = \frac{3}{2}\sigma_{\text{HEL}}(1 - c_b^2/c_l^2). \tag{2}$$

After the compression pulse is reflected from the free surface, tensile stresses are generated inside the sample,
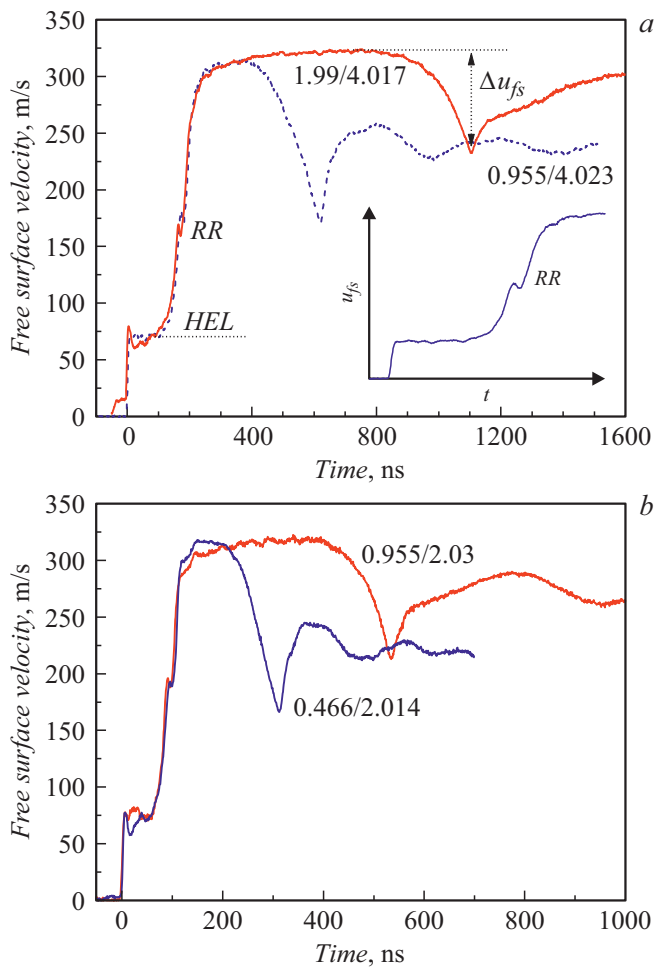
Figure 2. Free surface velocity profiles of Mn2-Si steel samples with a nominal thickness of 4 (*a*) and 2 mm (*b*). The numbers of the profiles show the actual values of the thickness of the copper pin and the sample. The insertion of the figure (*a*) shows the frontal part of the wave profile, which clearly shows the re-reflection of the elastic wave RR from the plastic shock wave. HEL (Hugoniot Elastic Limit).

as a result of which its fracture is initiated — spallation. In this case, the relaxation of tensile stresses occurs and a compression wave (spall pulse) is formed, the output of which to the surface of the sample usually causes a second rise in its velocity or stops its fall in the unloading part of the incident compression pulse. The decrement of the surface velocity Δu_{fs} at its decline from the maximum to the value before the front of the spall pulse is proportional to the magnitude of the fracture stress — the spall strength of the material under these loading conditions. In the linear (acoustic) approximation, the value of the spallation strength σ_{sp} of the material is defined as [10]:

$$\sigma_{sp} = \frac{1}{2}\rho_0 c_b(\Delta u_{fs} + \delta), \qquad (3)$$

where δ — correction for the distortion of the velocity profile due to the difference in the velocities of the elastic

front of the spall pulse and the velocity of the plastic part of the incident rarefaction wave in front of it [4]. Directly from the comparison of wave profiles in Figure 2, it can be seen that the value of Δu_{fs} in experiments with a thick impactor is significantly less than in the experiment with a thin impactor. This difference, at least in part, is explained by the mentioned distortion of the wave profile during the propagation of perturbations from the spall plane to the free rear surface. In this formulation of experiments, the spallation occurs at a distance from the free surface, approximately equal to the thickness of the impactor. In the experiment with a thicker impactor, the zone of spall fracture is more distant from the rear surface and, accordingly, more distortion accumulates at a greater distance. In our calculations we also considered the nonlinearity of the compressibility of the material [10,12]. The thickness of the spall plate h_{sp} was estimated from the period of velocity fluctuations on the wave profile Δt as $h_{sp} = c_l \Delta t / 2$.

The presented wave profiles show additional steps *RR*, which appeared after the reflection of the elastic precursor from the free surface and the interaction of the resulting reflected elastic release wave with the plastic shock wave [14]. Such a re-reflection is not always observed,
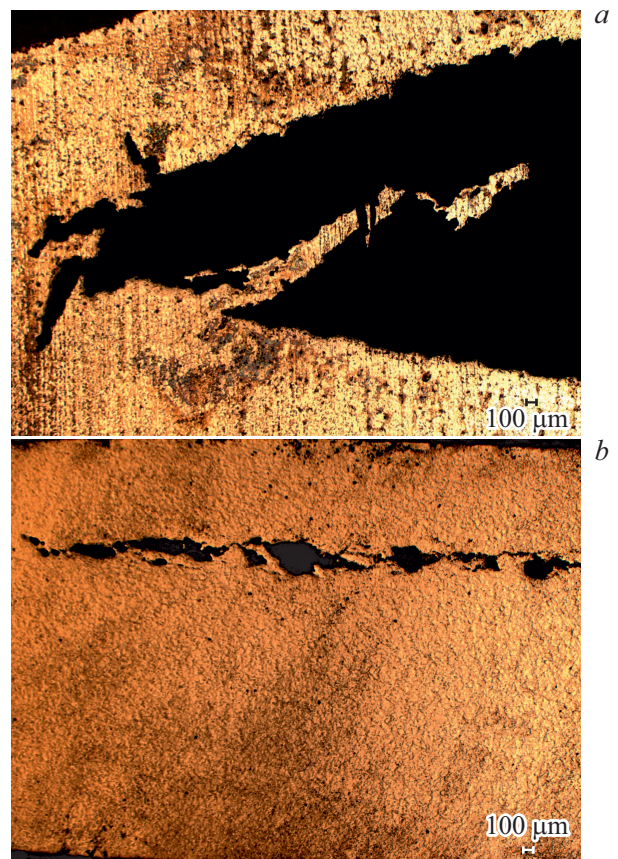
Figure 3. Micrographs of the peripheral parts of the cross sections of steel samples with a thickness of 4 mm after the experiments shown in Figure 2: *a* — when loaded with 2 mm pin (×25), *b* — when loaded with 0.96 mm pin.
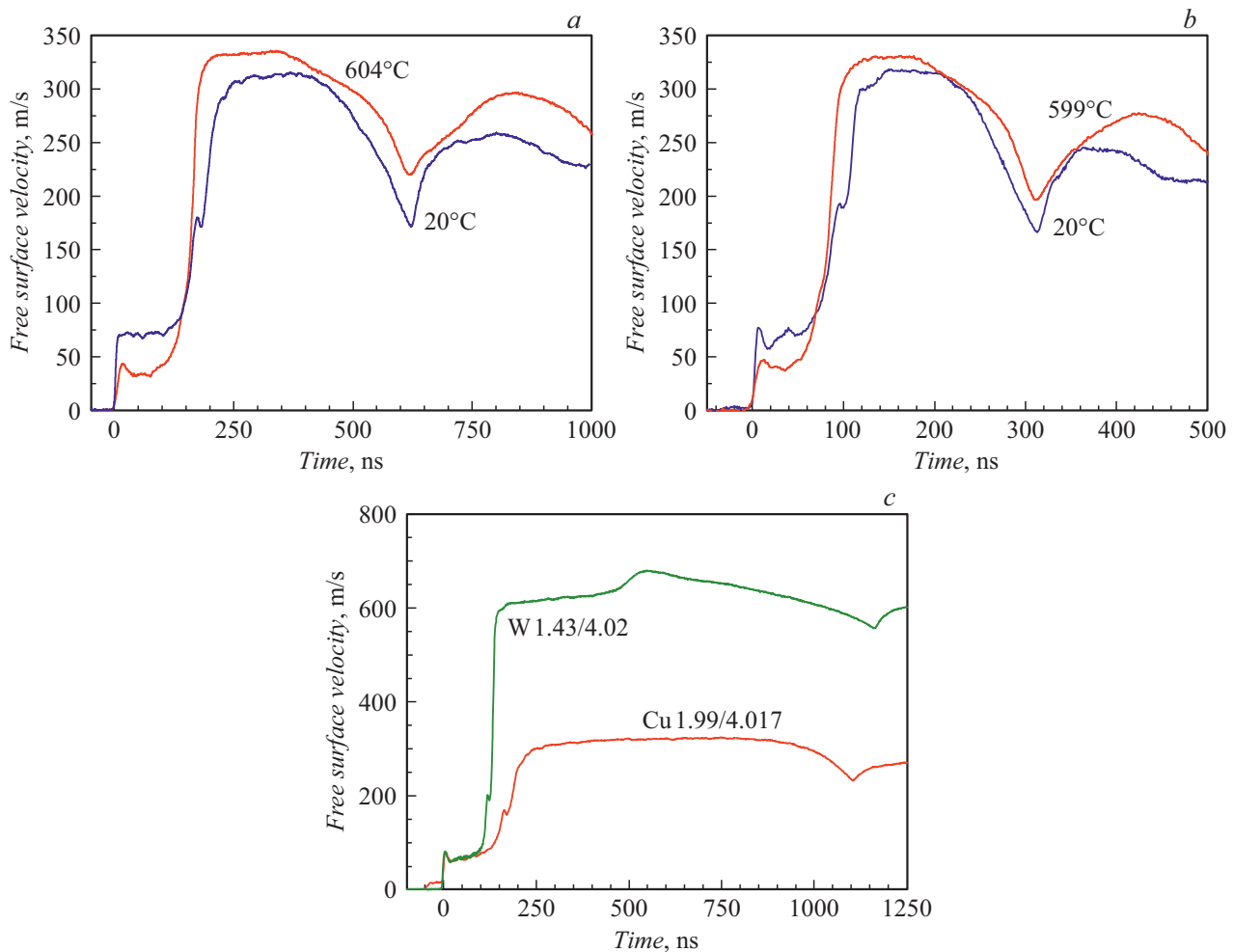
Figure 4. Results of experiments with samples of Mn2-Si steel: *a* — velocity profiles of the free surface of samples with a nominal thickness of 4 mm at normal and elevated temperatures, the experimental conditions correspond to points 1 and 14 of Table. 2; *b* — the same for thickness 2 mm, the experimental conditions correspond to points 3 and 15 of the Table. 2; *c* — profiles obtained at impact velocities of 340 ± 10 m/s and 590 ± 20 m/s, the conditions correspond to points 2 and 13 of Table 2.

the possibility of its formation, as well as the amplitude of the re-reflected wave and its decay are associated with the relaxation properties of the material in the state before the plastic shock wave. This feature and its details for Mn2-Si steel are discussed in work [13].

The photographs given in Figure 3 show that, depending on the kinetic energy reserve in the reclining plate, the spall fracture may have a different degree of completeness. In contrast to the fracture of one or several main cracks under normal conditions, the spall fracture occurs by the nucleation, growth and fusion of numerous cracks or pores with the formation of a developed fracture surface. It is more correct to talk about a zone of fracture of finite thickness, within which the fracture can have several localizations and form multiple spallation.

Figure 4, *a, b* compares the results of experiments with samples of Mn2-Si steel of nominal thickness 4 and 2 mm at elevated temperature with the results at room temperature.

In experiments at a collision velocity of 590 ± 20 m/s, the splitting of a plastic shock wave was recorded (Figure 4, *c*) due to the beginning of the well-known [14] polymorphic transformation $\alpha \to \varepsilon$ (BCC→HCP) when compressed. The pressure of the beginning of the transformation of steel, determined by the parameters of the first plastic shock wave, is 12.4 GPa, which is slightly lower than the pressure of the transformation of iron (13 GPa), and that is probably due to the presence of manganese in the steel. One can also note the increased amplitude of the re-reflected elastic wave *RR* in the experiment with a higher pressure of shock compression. For an ideal elastoplastic material with a constant yield strength, the amplitude of the re-reflected wave should not depend on the final pressure of the shock compression [14].

3.1. Spallation strength of Mn2-Si steel

Figure 5 summarizes the results of measurements of the shear strength of steel σ_{sp} in the form of its dependencies on the expansion rate of the substance $\dot{V}/V_0$ (deformation
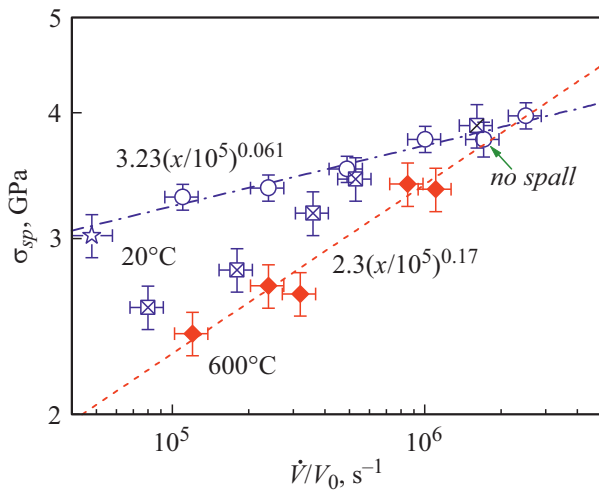
Figure 5. Dependence of the spall strength of Mn2-Si steel on the deformation rate in the rarefaction wave of the incident compression pulse. Open circles show the results of experiments with thin pins at room temperature, squares — results of experiments with thick pins, diamonds — results of high-temperature measurements, an asterisk shows the result of an experiment with polymorphic transformation $\alpha \to \varepsilon$.

rate) in the rarefaction wave before the shear pulse, which was defined as

$$\frac{\dot{V}}{V_0} = \frac{\dot{u}_{fsr}}{2c_0}, \qquad (4)$$

where $\dot{u}_{fsr}$ — the deceleration rate of the surface ahead of the spall pulse front, c_0 — the first term of the linear dependence $U_s - u_p$ (shock adiabatic), taking the value of the bulk sound speed at zero pressure. Earlier [15,16] it was shown that dependences of this kind are transformed depending on the rate of destruction (the rate of growth of the volume of discontinuities) from the stress. The graph in Figure 5 has the following specific features that distinguish the behavior of Mn2-Si steel from other metals and alloys. At strain rates less than $5 \cdot 10^5\,\mathrm{s}^{-1}$ there is a large discrepancy in the values of the spall strength obtained in experiments with thin and thick impactors. For other materials, similar processing of similar wave profiles, considering their fracture in accordance with the ratio (3), did not give a large difference in the results beyond the natural error. With an increase in the strain rate, i.e. with the transition to increasingly thin samples, this discrepancy gradually disappears. At the same time, the difference in the values of the spall strength at room temperature and at $600°C$ also decreases. All experiments at elevated temperatures were carried out with thin impactors, since such an experimental setup is associated with the least distortion of the wave profiles. It can be seen from Figure 5 that the measurement results covering more than one order of strain rates are approximated with acceptable accuracy by power dependences

$$\sigma_{sp} = 3.23\left(\frac{\dot{V}/V_0}{\dot{\varepsilon}_0}\right)^{0.061} \quad \text{at room temperature,} \qquad (5)$$

$$\sigma_{sp} = 2.3\left(\frac{\dot{V}/V_0}{\dot{\varepsilon}_0}\right)^{0.17} \quad \text{at } 600°C, \qquad (6)$$

where $\dot{\varepsilon}_0 = 10^5\,\mathrm{s}^{-1}$.

Figure 6 shows microphotographs of the diametrical cross section of samples stored after measurements at room and elevated temperatures with different magnifications. It can be seen that at room temperature, destruction occurs by the formation and growth of sharp cracks, and at high temperature, rounded pores in large quantities form instead of cracks in the material. The growth of round pores is associated with a lower stress concentration. Lower values of the spall strength and yield strength led to a more complete separation of the spall plate.

In Figure 7, the measurements results of the spallation strength of Mn2-Si steel are compared with similar data for Armco iron [17] and for reactor steel 15X2NMFA [4]. The weaker dependence of the spallation strength of Mn2-Si steel on the strain rate has led to the fact that at relatively small values of $\dot{V}/V_0$ it is close to the strength of reactor steel, and at large — to the strength of iron. This fact is likely a consequence of the presence of different spectra of potential foci of nucleation of fracture in these three materials.

3.2. Decay of the elastic precursor and initial rate of plastic deformation of Mn2-Si steel

Table 2 presents experimental conditions with Mn2-Si steel samples with a thickness from 0.17 to 4 mm at various temperatures and the results of their processing. Here T — initial temperature of the sample; h_{imp} — thickness of the pin (its material is also indicated); u_{imp} — impact velocity; h_{cm} — thickness of the sample; σ_{HEL} — Hugoniot elastic limit; σ_T — dynamic yield strength; σ_{sp} — spall strength; $\dot{V}/V_0$ — the rate of expansion when unloading the material from the shock-compressed state.

Figure 8 summarizes the results of measurements of compression stresses in an elastic precursor depending on the distance traveled by the wave (sample thickness) at room temperature and at $600°C$. At room temperature, at distances up to about 1 mm, there is an obvious decay of the precursor; at $600°C$, decay is recorded in the entire studied range of sample thicknesses. A similar transition from fast to slow decay was also observed for other metals with a volume-centered cubic structure and interpreted as a consequence of the transition from the over-barrier movement of dislocations controlled by phonon viscosity to thermal activation mechanisms for overcoming barriers at high voltages. The decay of the elastic precursor (shock compression waves) occurs due to stress relaxation and is associated with the rate of plastic deformation behind its front $\dot{\gamma}_p = (\dot{\varepsilon}_x^p - \dot{\varepsilon}_y^p)/2$ by the ratio [18]:

$$\left.\frac{d\sigma_x}{dh}\right|_{HEL} = -\frac{4}{3}\frac{\dot{\gamma}_p}{c_l}, \qquad (7)$$
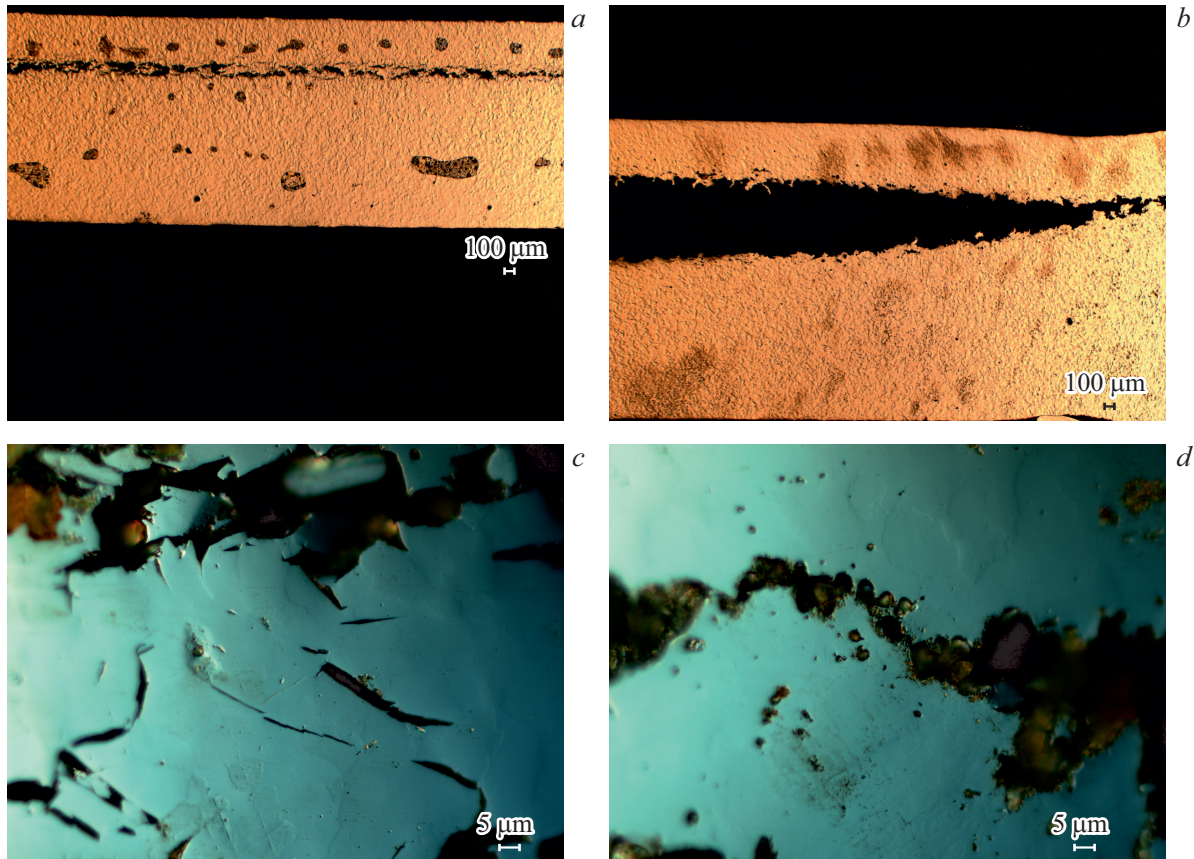
Figure 6. Micrographs of the split section at room temperature (a, c) and 599°C (b, d); a, b — magnification $(\times 25)$; c, d — magnification $(\times 1000)$.

where h — the distance traveled by the wave, G — the shear modulus, c_l — the propagation velocity of the precursor front, assumed in this approximation to be equal to the longitudinal sound speed. As for other metallic materials [3,15], the initial section of the empirical
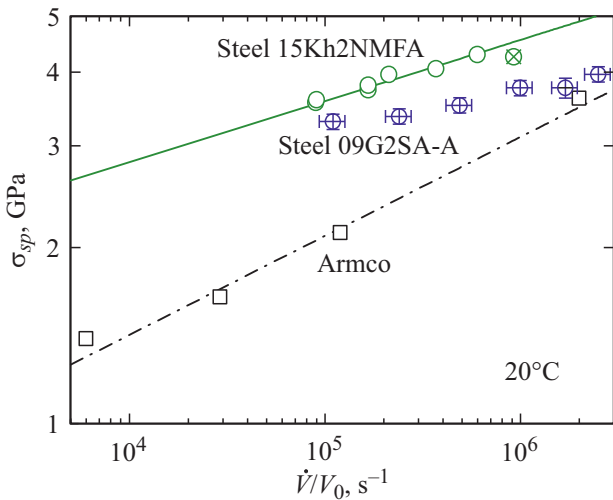
Figure 7. Comparison of the results of measurements of the spallation strength of Mn2-Si steel with data for Armco iron [12] and for reactor steel 15X2NMFA [13].
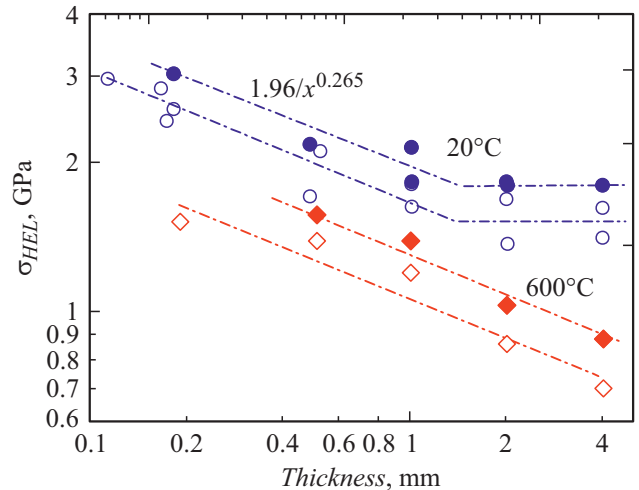
Figure 8. Decay of the elastic precursor in Mn2-Si steel at room temperature (circles) and at 600°C (diamonds). The open symbols correspond to the parameters at the minimum between the elastic and plastic waves, filled with — parameters at the peak of the elastic precursor.

dependence is approximated by a power function

$$\sigma_{\text{HEL}} = S(h/h_0)^{-\alpha}, \qquad (8)$$

Table 2. Experemental setup and results of experiments with Mn2-Si steel

№	T, °C	h_{imp}, mm	u_{imp}, m/s	h_{sm}, mm	σ_{HEL}, GPa*	σ_T, GPa	σ_{sp}, GPa	$\dot V/V_0$, s^{-1}	h_{sp}, mm
1	20	Cu 0.96	340 ± 10	4.02	1.62	0.93	3.3	$1.1 \cdot 10^5$	1.09
2	20	Cu 1.99	340 ± 10	4.02	1.8; 1.41	1.04; 0.81	2.56	$0.8 \cdot 10^5$	2.34
3	20	Cu 0.47	340 ± 10	2.01	1.83; 1.69	1.05; 0.97	3.37	$2.4 \cdot 10^5$	0.52
4	20	Cu 0.96	340 ± 10	2.03	1.8; 1.37	1.04; 0.79	2.79	$1.8 \cdot 10^5$	1.1
5	20	Cu 0.25	340 ± 10	1.015	2.15; 1.81	1.24; 1.04	3.52	$4.9 \cdot 10^5$	0.28
6	20	Cu 0.47	340 ± 10	1.017	1.83; 1.63	1.05; 0.94	3.18	$3.6 \cdot 10^5$	0.54
7	20	Cu 0.14	340 ± 10	0.527	2.11	1.22	3.77	10^6	0.16
8	20	Cu 0.28	340 ± 10	0.488	2.18; 1.71	1.26; 0.98	3.44	$5.3 \cdot 10^5$	0.29
9	20	Cu 0.044	340 ± 10	0.167	2.83	1.63	3.98	$2.5 \cdot 10^6$	0.058
10	20	Cu 0.094	340 ± 10	0.183	3.03; 2.57	1.75; 1.48	3.89	$1.6 \cdot 10^6$	0.11
11	20	Cu 0.046	340 ± 10	0.174	2.43	1.5	3.77**	$1.7 \cdot 10^6$	–
12	20	Cu 0.2	340 ± 10	0.114	2.96	1.7			–
13	20	W 1.43	590 ± 20	4.02	1.6	0.97	3.02	$4.8 \cdot 10^4$	2.6
14	604	Cu 0.96	340 ± 10	4.04	0.88; 0.7	0.49; 0.39	2.41	$1.2 \cdot 10^5$	1.08
15	599	Cu 0.48	340 ± 10	2.02	1.03; 0.86	0.57; 0.48	2.68	$2.4 \cdot 10^5$	0.52
16	598	Cu 0.256	340 ± 10	1.01	1.39; 1.2	0.77; 0.66	2.64	$4.9 \cdot 10^5$	0.31
17	604	Cu 0.133	340 ± 10	0.513	1.57; 1.39	0.87; 0.77	3.4	$8.5 \cdot 10^5$	0.16
18	603	Cu 0.097	340 ± 10	0.192	1.52	0.84	3.36	$1.1 \cdot 10^6$	0.12

N o t e . * top line — stress at the peak of the precursor, bottom — at the minimum point between elastic and plastic waves. ** assessment from below, there was no spall fracture.

where the parameter $h_0 = 1\,\text{mm}$. With a significant spread of experimental data, the indicator α for all their groups can be taken the same, equal to 0.265, and the values of the coefficient S vary from $S_{peak} = 1.96\,\text{GPa}$ for stress peaks and $S_{\min} = 1.67\,\text{GPa}$ for the minimum points between elastic and plastic waves at room temperature up to $S_{peak} = 1.3\,\text{GPa}$ and $S_{\min} = 1.07\,\text{GPa}$ at 600°C. The relatively small value of the indicator α is characteristic of metals and steels with a volume-centered cubic structure.

The empirical dependence (8) is transformed into the dependence of the initial velocity of plastic deformation on the shear stress τ:

$$\dot\gamma_P = \frac{3}{4}\left(\frac{\tau E'}{SG}\right)^{\frac{\alpha+1}{\alpha}}, \qquad (9)$$

where $E' = \rho_0 c_l^2$ — the modulus of longitudinal elasticity, G — the shear modulus. The dependences of the initial shear strain rate on the shear stress calculated in this way at room temperature at the fast attenuation site and at 600°C are shown in Figure 9. The graph also roughly shows the transition to a low-speed mode at room temperature.
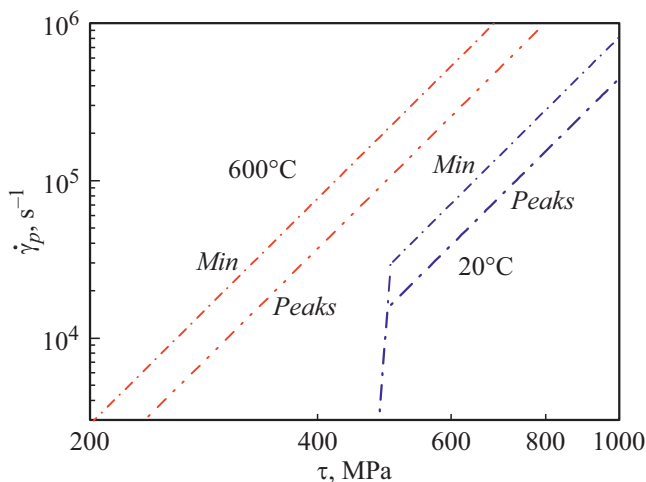
Figure 9. The dependence of the initial shear strain rate on the shear stress in the elastic precursor. Calculations are performed for the peak at the precursor front and for the minimum point between elastic and plastic waves.

Conclusion

According to the results of measurements of the velocity profiles of the free surface of samples of low-alloy ferrite-pearlite Mn2-Si steel of various thicknesses, the dependences of the resistance to deformation and fracture of the material on the strain rate and temperature are determined, which can later be used in the construction of mathematical models and govening ratios. At room temperature, a change in the main mechanism of inhibition of dislocations is recorded, which manifests itself in slowing down the decay of an elastic wave. At 600°C, the mechanism change occurs outside the investigated range of parameters of the evolution of the elastic-plastic shock compression wave. The stress of the plastic flow of shock-compressed steel was estimated at 600°C; it was found that after high-rate deformation in the shock wave, the stress of the plastic flow of steel is $2-2.5$ times less than the initial value in the elastic precursor. The pressure of the beginning of polymorphic transformation is determined $\alpha \rightarrow \varepsilon$ Mn2-Si steel under shock compression, which turned out to be slightly lower than in pure iron, which is explained by the presence of manganese in the steel. An unusual effect of the duration of the initial shock compression pulse was found, which manifests itself at relatively low strain rates.

Funding

Conflict of interest

The authors declare that they have no conflict of interest.

References

[1] V.I. Gorynin, M.I. Olenin. *Puti povysheniya khladostoykosti staley i s varnykh soedineniy* (FGUP TsNII KM „Prometei", SPb, 2017) (in Russian).
[2] V.A. Ryzhansky, A.G. Ivanov, V.V. Zhukov, V.N. Mineev. Atomnaya energetika, **79**, 3 (178) (in Russian).
[3] G.V. Garkushin, G.I. Kanel, S.V. Razorenov, A.S. Savinykh. Mechan. Sol., **52** (4), 407 (2017). DOI: 10.3103/S0025654417040070
[4] G.I. Kanel, G.V. Garkushin, A.S. Savinykh, S.V. Razorenov, S.A. Atroshenko. Tech. Phys., **65** (3), 420 (2020). DOI: 10.1134/S1063784220030111
[5] E.B. Zaretsky, G.I. Kanel, S.V. Razorenov, K. Baumung. Int. J. Impact Eng., **31** (1), 41 (2005). DOI: 10.1016/j.ijimpeng.2003.11.004
[6] L.M. Barker, R.E. Hollenbach. J. Appl. Phys., **45** (11), 4872 (1974). DOI: 10.1063/1.1663148
[7] D.J. Dever. J. Appl. Phys., **43**, 3293 (1972). DOI: 10.1063/1.1661710
[8] E.B. Zaretsky. J. Appl. Phys., **106**, 023510 (2009). DOI: 10.1063/1.3174442
[9] L.M. Barker, R.E. Hollenbach. J. Appl. Phys., **43**, 4669 (1972). DOI: 10.1063/1.1660986
[10] G.I. Kanel, S.V. Razorenov, A.V. Utkin, V.E. Fortov. *Udarno-volnoviye yavleniya v kondensirovannykh sredakh* (Janus-K, M., 1996) (in Russian).
[14] G.I. Kanel, *Udarnye volny v fizike tverdogo tela* (Fizmatlit, M., 2018) (in Russian).
[12] G.I. Kanel. J. Appl. Mechan. Tech. Phys. **42**, 358 (2001). DOI: 10.1023/A:1018804709273
[13] G.I. Kanel, A.S. Savinykh, G.V. Garkushin, S.V. Razorenov. Dokl. Phys., **66** (2), 35 (2021) DOI: 10.1134/S1028335821020038
[14] G.E. Duvail, R.A. Graham. Rev. Modern Phys., **49** (3), 523 (1977). DOI: 10.1103/RevModPhys.49.523
[15] T. Antoun, L. Seaman, D.R. Curran, G.I. Kanel, S.V. Razorenov, A.V. Utkin. *Spall Fracture* (Springer, NY., 2003)
[16] G.I. Kanel, S.V. Razorenov, A. Bogach, A.V. Utkin, D.E. Grady. Intern. J. Impact Eng., **20**, 467 (1997). DOI: 10.1016/S0734-743X(97)87435-0
[17] G.I. Kanel, S.V. Razorenov, G.V. Garkushin, S.I. Ashitkov, P.S. Komarov, M.B. Agranat. Physics Solid State, **56** (8), 1569 (2014). DOI: 10.1134/S1063783414080113
[18] G.E. Duvall. In: *Strss Waves in Anelastic Solids*, edited by H. Kolsky, W. Prager (Springer-Verlag, Berlin, 1964), p. 20. DOI: 10.1007/978-3-642-88288-3_2